JOURNAL OF GEOPHYSICAL RESEARCH, VOL. 106, NO. C11, PAGES 26,805–26,815, NOVEMBER 15, 2001

# Global patterns of decadal-scale variability observed in sea surface temperature and lower-tropospheric circulation fields

Tomohiko Tomita[1] and Bin Wang
International Pacific Research Center, University of Hawaii at Manoa, Hawaii, USA

Tetsuzo Yasunari[2]
Institute of Geoscience, University of Tsukuba, Tsukuba, Japan

Hisashi Nakamura[2]
Department of Earth and Planetary Physics, University of Tokyo, Tokyo, Japan

**Abstract.** The global patterns associated with decadal-scale variability (DSV) are examined by a lag correlation technique based on local anomaly indices, using the fields of measured sea surface temperature (SST) and 850 hPa geopotential height for the last 50 years. The three dominant patterns are identified, and the variability is examined; the first spreads over the entire Pacific, which is concurrent with the decadal-scale modulation of the El Niño/Southern Oscillation (DES variability), the second is confined to the local midlatitude North Pacific (LNP variability), and the third extends over the North Atlantic with the decadal North Atlantic Oscillation (NAO) (DNA variability). The global SST pattern of DES variability exhibits large-scale equatorial symmetry in the Pacific, which is similar to that of the Pacific Decadal Oscillation but is distinguished by the signals in the subtropical frontal zones. These SST anomalies are accompanied by anomalous subtropical highs that appear prior to the anomalous depression around Australia. The LNP variability, which is related with the Arctic Oscillation, is characterized by the SST anomalies along the North Pacific subarctic frontal zone moving eastward accompanied by the anomalous Aleutian Low. This variability develops (decays) without (with) coherent variability in the tropics. It shows the 6-year quadrature phase relationship with the DES variability, indicative of an interdecadal variability with a period of 24 years. The DNA variability is featured by the atmospheric NAO and by the SST anomalies in four zonal bands that spread in the North Atlantic from the tropics to high latitudes. This variability is independent of either the DES or LNP variability.

## 1. Introduction

Global climate variability on decadal and longer timescales is a subject of increasing scientific interest and relevance. A large number of researchers in the last decade have explored various climate variability with periods longer than interannual timescales [e.g., *Trenberth and Hurrell*, 1994; *Deser and Blackmon*, 1995; *Minobe*, 1997; *Nakamura et al.*, 1997; *Zhang et al.*, 1997; *White and Cayan*, 1998; *Xie and Tanimoto*, 1998]. These long-period climate variations may modulate shorter intraseasonal, seasonal, and interannual variability [*Wang*, 1995; *Balmaseda et al.*, 1995; *Wang and Wang*, 1996; *Goddard and Graham*, 1997; *Slingo et al.*, 1999; *An and Wang*, 2000] and may also obscure long-term climatic trends or global warming signals [*Latif et al.*, 1997]. It is therefore of great scientific importance to identify such long-period climate variability in a "global" perspective.

In the global ocean, two dominant spatial patterns of decadal-scale variability (DSV) have been identified; one is the so-called Pacific Decadal Oscillation (PDO) pattern [*Mantua et al.*, 1997], which is somewhat similar to that of the interannual El Niño/Southern Oscillation (ENSO) variability with equatorial symmetry in the entire Pacific [*Nitta and Yamada*, 1989; *Trenberth*, 1990; *Trenberth and Hurrell*, 1994; *Zhang and Wallace*, 1996; *Kachi and Nitta*, 1997; *White and Cayan*, 1998; *Zhang et al.*, 1998], and the other is the decadal North Atlantic Oscillation (NAO) pattern characterized by standing dipole structure of the anomalous Azores High and Icelandic Low [*Deser and Blackmon*, 1993; *Kushnir*, 1994; *Xie and Tanimoto*, 1998; *Watanabe et al.*, 1999]. *Kawamura* [1994] and *Deser and Blackmon* [1995] found an inherent DSV being locally dominant along the subarctic frontal zone (SAFZ) in the North Pacific and linearly independent of the interannual ENSO variability. *Nakamura et al.* [1997] and *Nakamura and Yamagata* [1999] also isolated it from the PDO.

Some significant decadal scale periods have already been detected in global climate variability [e.g., *Ghil and Vautard*, 1991; *Mann and Park*, 1994]. The DSV with a period of 15–20 years, which appears in global mean temperature [*Ghil and Vautard*, 1991; *Kang*, 1996], has a spatial pattern similar to that of interannual ENSO variability [*Mann and Park*, 1993, 1994; *Kang*, 1996], indicating the PDO. The 10- to 12-year variability

[1]Now at Frontier Research System for Global Change, Institute for Global Change Research, Yokohama, Japan.
[2]Also at Frontier Research System for Global Change, Institute for Global Change Research, Yokohama, Japan.



Paper number 2000JC000619.
0148-0227/01/2000JC000619$09.00

is dominant locally in the North Atlantic [*Mann and Park*, 1994], which corresponds to the decadal NAO [*Deser and Blackmon*, 1993; *Hurrell*, 1995; *Watanabe et al.*, 1999]. The quasiperiodic 10-year variability has also been detected along the North Pacific SAFZ [*Nakamura et al.*, 1997] with the superimposed interdecadal trend from the late 1950s to late 1980s [*Kawamura*, 1994; *Deser and Blackmon*, 1995]. The present work focuses on DSV with periods longer than 7 years that can capture at least the significant decadal variations mentioned above. The periodicity longer than 50 years, (e.g., the penta-decadal [*Mann and Park*, 1994; *Minobe*, 1997] or secular [*Mann and Park*, 1994] variability and the longer variation tendency [*Ghil and Vautard*, 1991]), however, cannot be resolved because the data period used in this work is too short.

In many of the previous studies a family of empirical orthogonal function (EOF) analysis such as conventional, rotated, and complex EOF analyses, or singular value decomposition analysis were used to identify the spatiotemporal structure of DSV [e.g., *Deser and Blackmon*, 1993; *Nakamura et al.*, 1997; *Tourre et al.*, 1999]. These methodologies may somewhat artificially emphasize standing or propagating features over a prescribed region with large variance, even if we apply an orthogonal rotation (e.g., the varimax rotation) to the several leading EOF modes [*Cheng et al.*, 1995]. In particular, as *Nakamura and Yamagata* [1998] pointed out, a conventional EOF analysis applied to a global or basin-wide field tends to extract a widespread variability over the tropics as the first mode and may fail to identify smaller but equally significant signals of DSV in coastal regions and/or the extratropical oceanic frontal zones. Furthermore, dominant patterns extracted through such a EOF analysis may be contaminated by contribution from data sparse regions because the covariance or correlation matrix is estimated from combination of all data in the analysis domain. Results of EOF analysis are sensitive to the size and location of an analysis domain. Some previous studies [*Deser and Blackmon*, 1993, 1995; *Nakamura et al.*, 1997; *Nakamura and Yamagata*, 1999] were confined to the analysis domain in specific ocean basins to reduce such artifacts. Yet arbitrariness still exists in choosing a localized analysis domain for EOF analysis. On the other hand, case studies such as a comparison between the two decades of 1965–1976 and 1977–1988 [e.g., *Nitta and Yamada*, 1989] may show the global patterns of DSV. The results, however, should not be robust until more realizations (i.e., events) are incorporated over a longer data period. We need to bridge a gap between the results of such EOF analyses and case studies to show more reliable and detailed structure of DSV in the global ocean-atmosphere field.

The purposes of the present work are to identify (1) "centers of action" of DSV in the global ocean, where observed decadal-scale sea surface temperature (SST) fluctuations are particularly large, (2) the temporal SST variation at each of the centers associated with DSV, and (3) the time evolution of the spatial patterns associated with those SST variations in the centers of action and the associated atmospheric variability as they appear in the global lag correlation maps. Specific focal points in this work are whether the Pacific DSV exhibits any coherence with the Atlantic DSV and whether the DSV in the midlatitude North Pacific exhibits any lagged relationship with that in the tropical Pacific. The results obtained from our analysis may facilitate validation of the model simulated DSV.

The data and methodology used in the present work are described in section 2. Major centers of action of DSV are identified, and these decadal variations are compared in section 3. Section 4 describes the global correlation patterns of DSV in terms of the time evolution with respect to those centers of action as identified in section 3. The general discussion and summary are given in section 5.

## 2. Data and Methodology

The data set used in the present work consists of monthly mean SST compiled at the UK Met Office [*Rayner et al.*, 1996], given on a $1° \times 1°$ grid covering the global oceans, in which the unobserved missing data have been reconstructed from a weighted linear sum of covariance EOFs with correspondingly adjusted time coefficients as the weights. Thus the global data are available for the entire period from 1903 to 1997. In the present work, however, the data only from 1949 to 1997 (49 years) are used because the reconstruction for this period has been based on high quality controlled observations (MOHSST6 [*Parker et al.*, 1995]). We also employ global 850 hPa geopotential height (Z850) data based on the National Center for Environmental Prediction/National Center for Atmospheric Research reanalyses, suited for examining lower tropospheric circulation. The data are available monthly for the period 1949–1997 (49 years) and a $2.5° \times 2.5°$ grid over the globe [*Kalnay et al.*, 1996].

In order to extract variation in SST and Z850 with periods longer than a year we first applied a 12-month running mean to their anomalies at each grid point that have been defined as the deviation from the long-term (49-year) mean of each month. Then we retained the averaged anomaly fields only for the 12-month periods from Aprils of individual years to Marches of the following years and another periods from individual Octobers to the following Septembers. These procedures yield the sequence of annual mean anomaly maps of the global SST and Z850 with half year intervals over the 49-year period. The resultant anomaly maps can capture continuous wintertime situations over the two hemispheres.

In the present work, DSV is defined and extracted from the annual mean anomaly time series from 1949 to 1997 through a harmonic analysis. The integrated harmonics of temporal wave numbers one through seven are regarded as the DSV, which include fluctuations with periods longer than 7 years. Since the smoothed time series has fewer degrees of freedom than the original one, we estimated the effective degrees of freedom using an autocorrelation technique [*Livezey and Chen*, 1983; *Fraedrich et al.*, 1995].

Autocorrelation and cross-correlation techniques are employed to examine the phase relationship among the specified time series. A significance test is then performed for the correlation coefficients using the two-tailed Student's $t$ test with the effective degrees of freedom estimated as above. We avoid employing more sophisticated power and cross-spectrum analyses that are based on Fourier transform of autocorrelation and cross-correlation functions because of the shortness of the data period. Since the record length is too short to extract general features of DSV in any robust way, the present work should be regarded as an extended case study of DSV.

## 3. Correlation Among the Centers of Action of DSV

In order to identify centers of action of DSV we first estimated the local standard deviation (SD) of DSV in the global SST (Figure 1). As apparent in Figure 1, shaded regions with

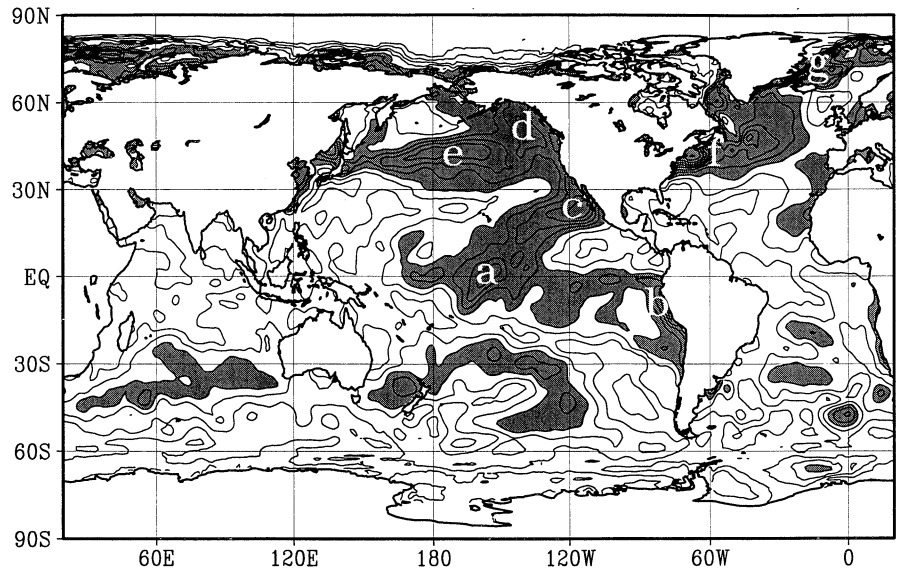


**Figure 1.** Global distribution of standard deviation of the SST DSV from 1949 to 1997. The contour interval is 0.05°C. Regions with values larger than 0.25°C are shaded. The centers of action of DSV are marked by seven labels (a–g), which correspond to those in Table 1.

SD larger than 0.25°C show a large-scale pattern with equatorial symmetry in the entire Pacific, which is somewhat similar to that of the interannual ENSO variability [e.g., *Nitta and Yamada*, 1989; *Trenberth and Hurrell*, 1994]. A close inspection, however, reveals that the SD of decadal SST variability is less confined to the equatorial eastern Pacific than that of the ENSO variability [e.g., *Kachi and Nitta*, 1997; *Zhang et al.*, 1997; *Zhang et al.*, 1998]. In fact, the equatorial maximum in the eastern Pacific, which characterizes the ENSO variability, is no longer distinctive in Figure 1.

Centers of action of DSV are defined in the present work with reference to the regions with particularly large SD of the decadal SST variability as shown in Figure 1. With the criterion of 0.35°C in SD, we can identify seven centers of action of DSV in the following regions: region a, the central equatorial Pacific; region b, off Peru; region c, the subtropical northeastern Pacific off Baja California; region d, near the Gulf of Alaska; region e, the midlatitude North Pacific; region f, off New England; and region g, around the Denmark Strait. The specific definitions of the individual centers are listed in Table 1. Hereinafter, a–g are used to represent the corresponding regions, unless otherwise noted.

In order to evaluate the contribution of DSV toward the total variance the variance ratio was estimated for the individual regions and is listed in Table 1. The ratios range from 25 to 80%, which are nonnegligible. The largest value, which exceeds 80%, is observed off New England (region f), and the large ratios are found in the regions f and g in the North Atlantic. The smaller ratios in the regions a and b in the tropical Pacific are due to the large contribution of the interannual ENSO variability in the regions a and b (variance 1 in Table 1). The modest ratios in regions c–e in the subtropical and extratropical Pacific, which range from 50 to 70%, are suggestive of the remote effects of interannual ENSO variability through the atmospheric teleconnection [*Horel and Wallace*, 1981; *Hamilton*, 1988; *Lau and Nath*, 1996] or through the coastally trapped internal waves off the west coast of North America [*Meyers et al.*, 1998].

Figure 2 shows the normalized annual-mean time series of unsmoothed anomalies (dotted lines) and the smoothed DSV (solid lines) individually averaged in the seven regions a–g (Table 1). The smoothed time series well capture the low-frequency fluctuation, especially in the time series f and g in the North Atlantic where DSV accounts for >70% of the total variance (Table 1). We can identify the large and coherent interannual ENSO variability in both time series a and b in the tropical Pacific. It appears that coherent variability exists

**Table 1.** Centers of Action of Decadal-Scale Variability[a]

| | Region | Longitude, Latitude | Variance 1 (Original Data), $\times 10^{-2}$ °C$^2$ | Variance 2 (Decadal Data), $\times 10^{-2}$ °C$^2$ | Ratio (Variance 2/ Variance 1 × 100), % |
|---|---|---|---|---|---|
| a | equatorial central Pacific | 165–145°W, 7.5°S to 7.5°N | 34.4 | 11.6 | 33.7 |
| b | off Peru | 90–70°W, 20°S to equator | 29.2 | 7.2 | 24.7 |
| c | off Baja California | 140–110°W, 17.5–27.5°N | 18.0 | 12.6 | 70.0 |
| d | Gulf of Alaska | 160–120°W, 50–60°N | 17.4 | 8.7 | 50.0 |
| e | mid-North Pacific | 160°E to 150°W, 37.5–45°N | 19.8 | 10.5 | 53.0 |
| f | off New England | 80–50°W, 35–47.5°N | 13.7 | 11.1 | 81.0 |
| g | Denmark Strait | 40–5°W, 65–77.5°N | 12.2 | 8.8 | 72.1 |

[a]Observed in the global SST field (Figure 1) and the contribution toward the total variance in each of the centers.

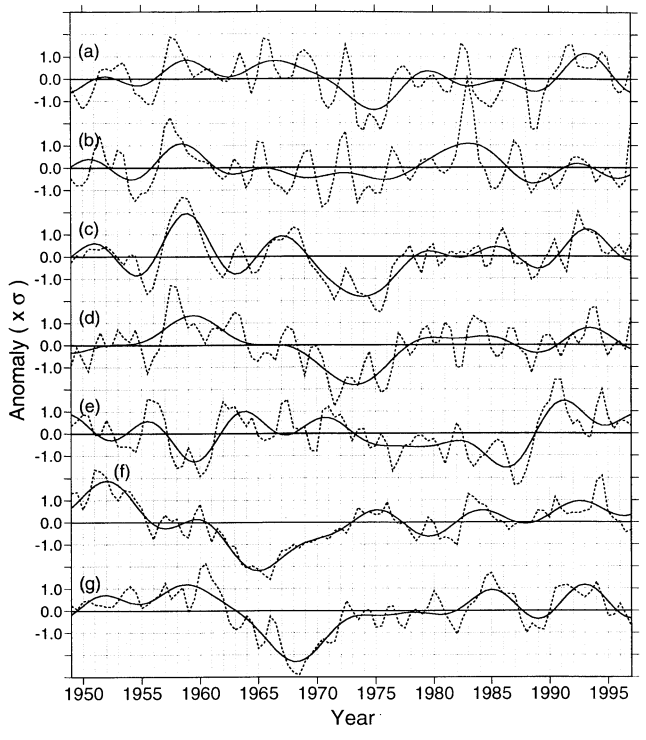


**Figure 2.** SST time series in the centers of action of DSV listed in Table 1. Dotted lines indicate the normalized time series of unsmoothed annual mean, while solid lines indicate the DSV component.

among the time series a–d in the Pacific and between the time series f and g in the North Atlantic.

In order to examine the linear relationship among the DSV time series in Figure 2 we show the simultaneous correlation coefficients for all of the combinations in Table 2, where the significant correlation at the 95% level is indicated by values in parentheses. The correlation coefficients are significant among the DSV time series in the equatorial central Pacific (region a), off Peru (region b), off Baja California (region c), and near the Gulf of Alaska (region d), with an exception of that between the time series a and b. A correlation coefficient is also large and significant between the DSV time series off New England (region f) and around the Denmark Strait (region g), as suggested earlier. The DSV in the midlatitude North Pacific (region e) shows no significant correlation with the others.

In this work, we avoid discussing a specific correlation between the DSV time series off Peru (region b) and around the Denmark Strait (region g) because none of DSV in other related regions (a, c, and d) exhibits a significant correlation with that in region g. Since the 95% significant level is dependent on the effective degrees of freedom included in each of the smoothed time series, the correlation between regions b and g is more significant than that between regions d and g even though the latter value is larger than the former one, reflecting stronger DSV persistency in region d than in region b (see Figure 2).

On the basis of these significant correlations we can divide the seven centers of action of DSV (Table 1 and Figure 1) into three groups and classify global DSV accordingly, i.e., (1) the DSV over the eastern half of the Pacific, (2) the local DSV confined to the midlatitude North Pacific, and (3) the DSV extending in the North Atlantic. The DSV in the Southern Oscillation index defined by the sea level pressure difference between Tahiti and Darwin (Tahiti-Darwin) shows the maximum significant correlation with that of group 1 at the lag zero, e.g., −0.67 with the smoothed time series off Baja California (region c). The DSV in the NAO index, which is an indicator of the anomalous surface westerlies between the Azores High and the Icelandic Low (Azores High–Icelandic Low), also shows the maximum significant correlation with that of group 3 with 1-year precedence of the NAO index, e.g., 0.54 with the smoothed time series off New England (region f). With these correlations we regard groups 1, 2, and 3 as the decadal ENSO (DES) variability, the local North Pacific (LNP) variability, and the decadal North Atlantic (DNA) variability relevant to the NAO, respectively. Hereinafter the DSV time series off Baja California (region c) is referred to as the representative indicator of the DES variability. The DSV time series in the midlatitude North Pacific (region e) and off New England (region f) are adopted to examine the LNP and DNA variability, respectively. The choice of these reference time series is based on both the large variance ratios in Table 1 and the significant correlation coefficients in Table 2.

Applying a conventional EOF analysis to the extratropical North Pacific SST in boreal winter, *Nakamura et al.* [1997] identified a spatial pattern similar to the DES variability in their second EOF, while the LNP variability may correspond to their first EOF or a mode identified by *Deser and Blackmon* [1995]. Applying the similar conventional EOF technique to the North Atlantic SST in boreal winter, *Deser and Blackmon* [1993] and *Watanabe et al.* [1999] detected the DSV widely extending in the North Atlantic as the DNA variability. Since a family of EOF analysis tends to capture a broad and smoothed anomaly pattern as the leading EOF [*Craddock and Flood*, 1969; *Weare et al.*, 1976], these earlier works may somewhat overlook the significance of regional SST anomalies such as variations confined to the regions off New England or around Denmark Strait (Figure 1). The large-scale decadal

**Table 2.** Simultaneous Correlation Coefficients (Decadal)[a]

| | a | b | c | d | e | f | g |
|---|---|---|---|---|---|---|---|
| a | | | | | | | |
| b | 0.34 | | | | | | |
| c | (0.82) | (0.59) | | | | | |
| d | (0.70) | (0.58) | (0.83) | | | | |
| e | 0.14 | −0.38 | −0.17 | −0.19 | | | |
| f | −0.29 | 0.11 | 0.04 | 0.01 | −0.09 | | |
| g | 0.06 | (0.49) | 0.31 | 0.53 | −0.25 | (0.62) | |

[a]Among the smoothed time series shown in Figure 2. Values in parentheses indicate the significant correlation coefficients at the 95% level, which are tested by the two-tailed Student's $t$ test using the effective degrees of freedom.

dipole in the tropical Atlantic, which was discussed, for example, by *Xie and Tanimoto* [1998] and *Robertson et al.* [2000], might be statistically emphasized by this analysis technique. In section 4 we examine the global patterns coherent with each of the DES, LNP, and DNA variability and the phase relationship among them.

## 4. Global Patterns of DSV

In order to examine global correlation patterns associated with the DES, LNP, and DNA variability classified in section 3, a lag correlation technique based on the smoothed reference time series off Baja California (region c), in the midlatitude North Pacific (region e), and off New England (region f) was applied to global SST and Z850 fields. Before calculating the lag correlation coefficients, the time series of SST and Z850 at each grid point have been smoothed through procedures similar to those applied to the time series in Figure 2. Since large lags result in loss of information near the ends of time series, only small lags from $-2$ to $+2$ years were imposed when computing the lag correlation coefficients in the global fields. An advantage of this correlation technique is that the spatial pattern would not be changed even if we excluded the region south of 30°S or confined the analysis domain to a specific ocean basin. In the following, we examine the evolution of the global correlation patterns and argue the anomaly fields inferred from the product with SD fields (see Figure 1) as a regression analysis.

Figure 3 shows the global correlation patterns in the SST and Z850 fields associated with the DES variability around the mature phase. Figure 3a–3e show the evolution in SST, while those in Figures 3f–3j exhibit the corresponding patterns in Z850. The patterns evolve from the top to the bottom. At the developing stage of the DES variability, a well-defined pattern with significant correlation gradually appears in the SST field particularly in the North and South Pacific subtropical frontal zones (STFZs), in the tropical central eastern Pacific through the eastern subtropical Pacific, and off the west coasts of the North and South American continents, with equatorial symmetry in the entire Pacific (Figures 3a and 3b) [cf. *Mantua et al.*, 1997; *White and Cayan*, 1998]. Concomitantly, in the Z850 field (Figures 3f and 3g), regions with significant negative correlation spread over the subtropical Pacific in the two hemispheres. The southern signals appear prior to the northern ones. This Z850 pattern corresponds to the weakened subtropical highs in conjunction with negative SST anomalies in the two Pacific STFZs. The associated weakening of the trades acts to maintain positive SST anomalies in the tropical central eastern Pacific. The weaker subtropical highs also relax the equatorward winds along the west coasts of the North and South American continents. The resultant weakening of the coastal upwelling acts to maintain positive SST anomalies along the coasts.

By the mature phase of the lag zero, other significant SST signals appear in the Indian Ocean and in the tropical North Atlantic (Figure 3c). The centers of action associated with the DES variability (a–d in Figure 1 and Table 1) are all situated in the regions where the local SST is significantly correlated with the SST off Baja California. It has been confirmed that a spatial pattern quite similar to that exhibited in Figure 3c is obtained when we adopt any of the smoothed time series a–d (Table 1 and Figure 2) as the reference time series (not shown). In the corresponding Z850 field (Figure 3h) the additional significant signals appear around Australia and in the tropical South Atlantic. A region with significant positive correlation to the north of the United States may reflect a remote atmospheric influence from the tropical western Pacific in the form of the stationary Rossby waves. The weakening of the trades associated with the positive Z850 correlations in the equatorial Atlantic acts to maintain the positive SST anomalies in the tropical North Atlantic (see Figure 3c). The positive Z850 signals over Australia and the negative ones over the subtropical high in the South Pacific, which correspond to the DSV in the Southern Oscillation [cf. *Trenberth and Shea*, 1987], constitute the atmospheric component of the decadal ENSO.

At the decay stage the positive SST signals gradually weaken and extend westward in the tropical Pacific (Figures 3d and 3e). The signals in Z850 exhibit the rapid weakening around the subtropical high in the South Pacific (Figures 3h–3j). By the lag of $+2$ years the negative Z850 signals almost disappear around the two Pacific STFZs, while part of positive signals still remain over Australia (Figure 3j). Unlike the PDO as identified by *Mantua et al.* [1997], the DES pattern does not show any significant SST and Z850 signals along the North Pacific SAFZ in the lags from $-2$ to $+2$ years.

Figure 4 shows the evolutionary tendency around the mature phase of the LNP variability. The positive SST correlation develops along the SAFZ in the North Pacific, concurrent with the development of positive Z850 correlation to the northeast near the climatological mean center of the Aleutian Low (Figures 4a–4c and 4f–4h). At the developing stage, there appear no significant signals in the tropical North Pacific in either the SST or Z850 field. As such, the development of the LNP variability is confined to the midlatitude North Pacific [*Latif and Barnett*, 1994; *Deser and Blackmon*, 1995; *Nakamura et al.*, 1997; *Nakamura and Yamagata*, 1999]. This result strongly suggests the existence of an air-sea coupling inherent in the midlatitude North Pacific, although the lag-correlation technique does not reveal any causal relationship of the decadal SST and Z850 variability.

By the mature phase a well-defined correlation pattern also emerges over the Arctic in the Z850 field (Figure 4h), suggesting the linkage to the Arctic Oscillation [*Thompson and Wallace*, 1998, 2000; *Wang and Ikeda*, 2000]. In fact, the representative time series e in the midlatitude North Pacific (Table 1 and Figure 2) shows a significant simultaneous correlation (0.52) with the smoothed Arctic Oscillation index at the 95% level (0.46), which is defined by the score time series for the leading EOF of the anomalous sea level pressure in the Northern Hemisphere [*Thompson and Wallace*, 1998]. Concomitantly, the significant correlation in the opposite sense develops over the Antarctica. The interhemispheric seesaw between the Arctic and the Antarctic through the LNP variability is, however, still a question for which further study is needed to shed light on the physical linkage. It is somewhat questionable whether the SST signals are meaningful in the midlatitude South Pacific because of the data quality there, although these may reflect the equatorial symmetry in the LNP variability.

By the decay stage the location of positive SST correlation, which is slightly shifted eastward along the SAFZ, is centered to the east of the dateline in the midlatitude North Pacific (Figures 4d and 4e). In the corresponding Z850 field (Figures 4i–4j) the negative correlation is strengthened in the tropical eastern Pacific concurrent with the weakening of positive correlation in the midlatitudes. It is suggested that the associated

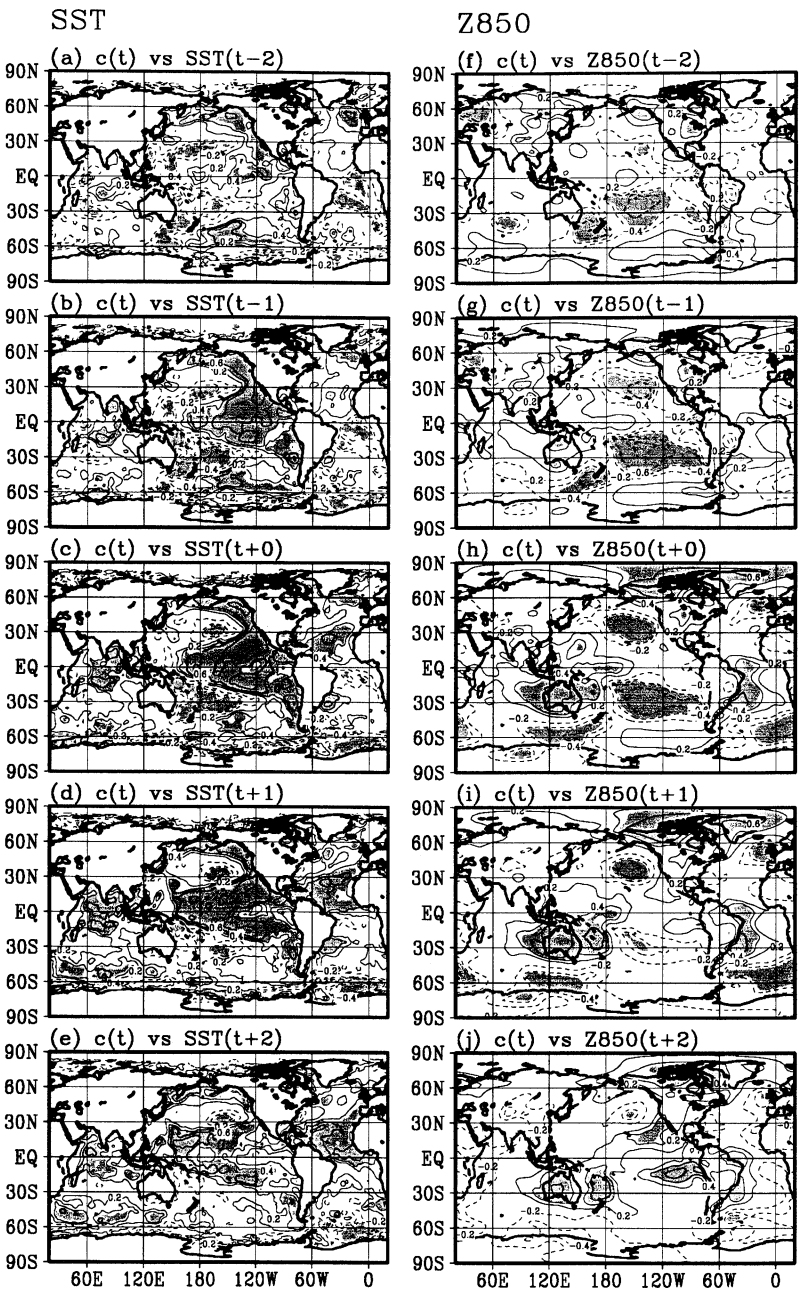


**Figure 3.** Global distribution of lag correlation coefficients in (left) SST and (right) Z850 associated with the DES variability. The lags are imposed from −2 to +2 years. Solid (dashed) lines indicate the positive (negative) correlation, and zero lines are omitted. The contour interval is 0.2. Areas where the correlation is significant at the 95% level are shaded.

tendency in anomalous winds may contribute to the weakening of positive SST correlation along the SAFZ and the slight southwestward extension from its eastern edge near 150°W, 45°N (Figures 4d and 4e). As *Latif and Barnett* [1994], *Zhang and Levitus* [1997], and *Tourre et al.* [1999] pointed out, the eastward movement of positive SST correlation along the SAFZ may manifest part of the decadal-scale advection of thermal anomalies along the North Pacific subtropical gyre.

Figure 5 shows the SST and Z850 patterns associated with the DNA variability and the evolutionary tendency around the mature phase. For the developing stage (Figures 5a–5c and 5f–5h), there appear to be well-defined correlation patterns over the North Atlantic in each of the SST and Z850 fields. The pattern in Z850 is characterized by the so-called NAO-like pattern, which is an anomalous pressure dipole between the Icelandic Low and the Azores High [*Wallace and Gutzler*, 1981; *Barnston and Livezey*, 1987; *Hurrell*, 1995]. Significant signals are also found over Europe and over northern South America. Whereas in the North Atlantic SST field, a "striped" pattern is pronounced that consists of the negative correlations in the tropical North Atlantic and to the east of the Labrador Sea and of the positive ones off New England and around the Norwegian Sea [*Deser and Blackmon*, 1993; *Kushnir*, 1994; *Watanabe et al.*, 1999]. These SST and Z850 patterns tend to remain in the following stages. In particular, the striped SST pattern persists at least until the lag of +2 years with slow eastward

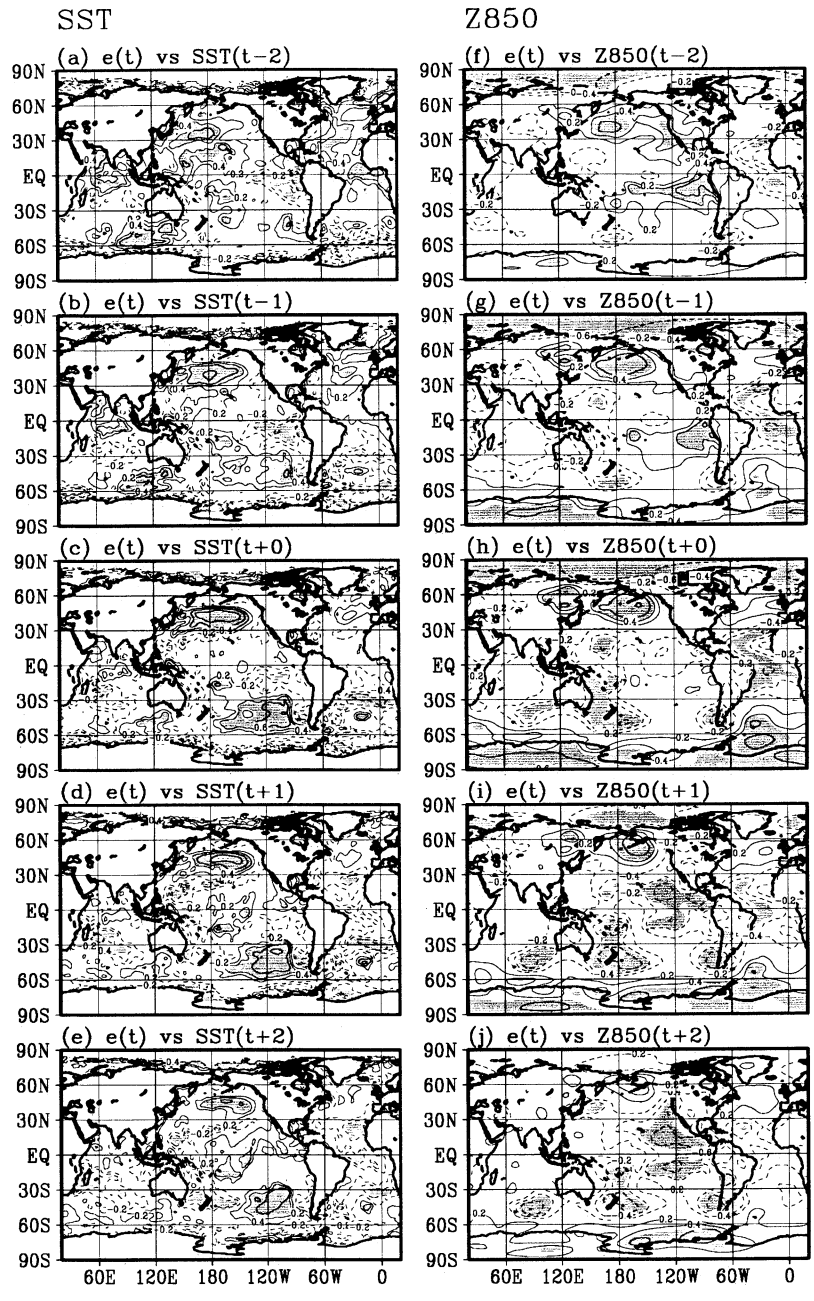


**Figure 4.** Same as Figure 3 except for the LNP variability.

expansion off New England (Figures 5a–5e) [*Sutton and Allen*, 1997].

The persistency of the atmospheric NAO-like pattern (Figures 5f–5j) is weaker than that of the striped SST pattern (Figures 5a–5e). The lag correlation maps appear to indicate a lag relationship between the SST variability and the atmospheric NAO with the lag of a few years as discussed in the earlier section using the NAO index and the time series f off New England (Table 1 and Figure 2). The atmospheric NAO might be more sensitive to the SST anomalies just off New England coast (Figures 5a and 5f) than those in the central North Atlantic (Figures 5e and 5j). If so, the slow eastward propagation of SST anomalies along the Gulf Stream path as found by *Sutton and Allen* [1997] could explain such a lag relationship.

On the basis of the reference time series c off Baja California, e in the midlatitude North Pacific, and f off New England (Table 1 and Figure 2), we examined the phase relationship among the DES, LNP, and DNA variability over a wide range of lags from −9 to +9 years (Figure 6). Note that the larger the lag is, namely, the smaller the degrees of freedom are, the less robustness the correlation has. In Figure 6a, significant correlation appears at the lags of −7 and +5 years. The former negative (latter positive) correlation indicates a tendency that the correlation pattern of the LNP variability (e.g., Figures 4c and 4h) with the opposite (same) sign appears prior (posterior) to that of the DES variability (e.g., Figures 3c and 3h) by about 7 (5) years. It may be regarded as the 6-year quadrature phase relation between the DES and LNP variability, which as a combination consists the interdecadal thermal advection along

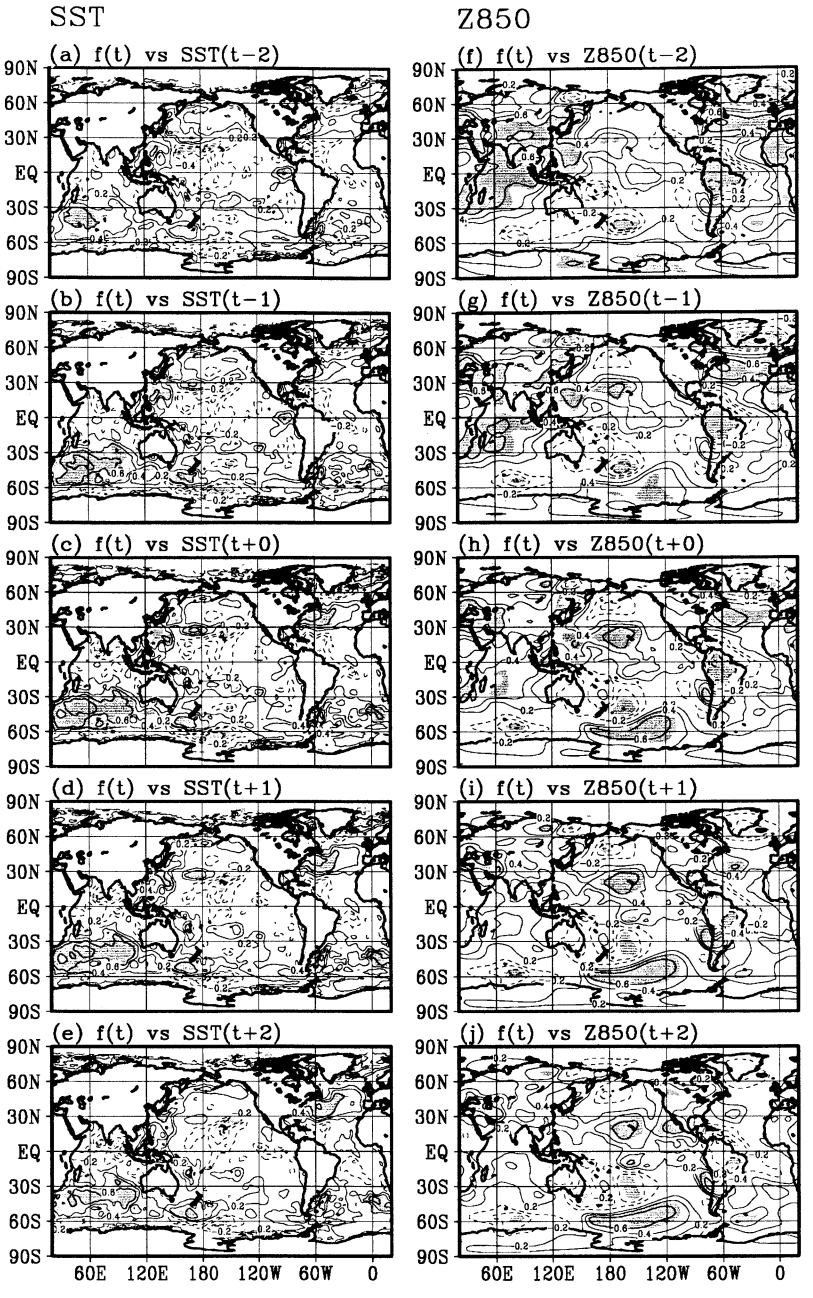


**Figure 5.** Same as Figure 3 except for the DNA variability.

the North Pacific subtropical gyre [*Latif and Barnett*, 1994; *Zhang and Levitus*, 1997; *Tourre et al.*, 1999].

The other significant correlation appears at the lags of +7 or +8 years in Figure 6c, indicating a tendency that the DES variability (e.g., Figures 3c and 3h) is lagged behind the DNA variability (e.g., Figures 5c and 5h) by ~7 years. This interbasin correlation seems to be questionable because the LNP variability, which has the 6-year quadrature phase relationship with the DES variability (Figure 6a), shows no significant correlation with the DNA variability (Figure 6b) and because the NAO index shows no significant correlation with the DES variability (not shown). Further study is need to examine the reality of this particular correlation between the DES and DNA variability.

## 5. Summary and Discussion

The global structure of decadal-scale variability (DSV) observed in the climate system in the late twentieth century has been examined through a lag correlation technique applied to sea surface temperature (SST) and 850 hPa geopotential height (Z850) fields. The lag correlation technique has an advantage in that its outcome is independent of a particular choice of the analysis domain. However, the present work should be still considered as an extended case study because the data record is obviously not long enough to extract the sufficient number of DSV events.

The following three patterns of DSV have been identified and depicted in the global SST and Z850 fields, i.e., (1) the

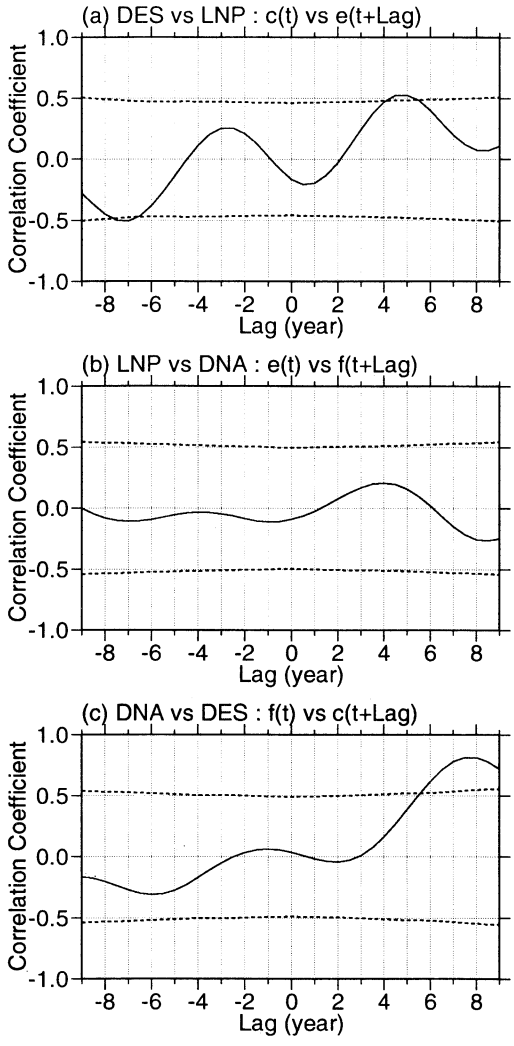


**Figure 6.** Correlation coefficients among the representative time series of DES (off Baja California, region c), LNP (in the midlatitude North Pacific, region e), and DNA (off New England, region f) variability for lags from −9 to +9 years. The 95% significant level is shown by dotted lines.

Pan-Pacific DSV, which is associated with the decadal-scale modulation of the El Niño/Southern Oscillation (ENSO) (DES variability), (2) the local DSV confined to the midlatitude North Pacific (LNP variability), and (3) the DSV in the North Atlantic being related to the North Atlantic Oscillation (NAO) (DNA variability).

The global correlation pattern of DES variability is characterized by coherent SST signals that cover almost the entire Pacific with equatorial symmetry [e.g., *White and Cayan*, 1998]. The pattern includes in-phase SST fluctuations between the tropics and high latitudes around 55° both in the North and South Pacific, which are in seesaw with those in the subtropical frontal zones (STFZs) in the two hemispheres. The tropical-subtropical seesaws in SST in the two hemispheres are accompanied by the anomalous subtropical highs and by the pressure anomalies in the opposite sense over Australia, indicative of the anomalous Walker circulation. The associated anomalies in the trades over the tropical Pacific and the meridional winds along the west coasts of the North and South American continents act to maintain the underlying SST anomalies via anomalous turbulent heat fluxes and anomalous coastal upwelling. The coherent remote effects of DES variability also appear in the Indian Ocean and the tropical Atlantic seemingly through an anomalous Walker cell in the tropics.

The SST fluctuations associated with the LNP variability tend to be confined to the North Pacific SAFZ, with very weak simultaneous correlation with the tropical Pacific SST. The corresponding atmospheric patterns are manifested as the anomalous Aleutian Low, again only with very weak simultaneous correlation in the tropical Pacific especially in the developing stage. The associated anomalous westerlies above the SAFZ are favorable to reinforce the SST anomalies there. An air-sea coupling local in the midlatitude North Pacific might be involved in the development and in the slow eastward movement along the SAFZ. On the other hand, the significant atmospheric signals appear in the tropical eastern Pacific in the decaying stage, suggesting a tropical-extratropical interaction.

Our correlation analysis clearly shows that the LNP variability is related to the Arctic Oscillation. The LNP variability exhibits the 6-year quadrature phase relation with the DES variability indicative of a coherent interdecadal variability with a period of ~24 years. Their representative spatial patterns (Figures 3c, 3h, 4c, and 4h) may manifest two extremes of the quasiperiodic interdecadal variability as explained through the subtropical ocean gyre circulation in the North Pacific [*Latif and Barnett*, 1994; *Zhang and Levitus*, 1997; *Tourre et al.*, 1999]. Further study is needed to identify the physical mechanisms connecting the DES and LNP variability.

The spatial patterns associated with the DNA variability are characterized by the atmospheric NAO and the concurrent striped SST anomalies in the tropical North Pacific, off the southeastern United States, east of the Labrador Sea, and in the Norwegian Sea [*Deser and Blackmon*, 1993; *Watanabe et al.*, 1999]. These SST anomalies tend to persist longer than the atmospheric NAO signals. Coherent atmospheric signals are also found over Europe and northern South America. The DNA variability is linearly independent of either the DES or LNP variability within small time lags <5 years.

Unlike most of the previous studies, where some sophisticated analysis methods such as empirical orthogonal function (EOF) or singular value decomposition analyses were used to identify the dominant spatiotemporal structure of DSV, an ad hoc method is used in the present work, that is, first locating regions of the strong DSV in the global SST field and then identifying the associated global patterns in both SST and Z850 fields based on a lag correlation technique for each of these regions. This ad hoc method has such advantages over those sophisticated methods as being free from the sensitivity of identified patterns to a particular choice of an analysis domain and also from artificially emphasizing either stationary or moving features in regions with large variance.

Signatures of the DES and LNP variability may be mixed up as a standing oscillation, for instance, the Pacific Decadal Oscillation (PDO) defined by the leading EOF of the basin-wide North Pacific SST [*Mantua et al.*, 1997]. The spatial pattern of PDO is distinguished from that of the DES variability with respect to whether or not the significant signals appear along the SAFZ. On the other hand, the LNP variability confined to the SAFZ is accompanied by no concurrent signals in the tropical Pacific. As pointed out by *Nakamura and Yamagata* [1998], a conventional EOF analysis applied to such a basin-wide field often fails to distinguish a locally dominant pattern from a basin-wide pattern.

A limitation of the present work obviously lies in the lag correlation technique wherein only small lags of ±1 and ±2 years were imposed in order to retain as many degrees of freedom as possible. Our analysis therefore can resolve the evolution tendency of DSV only for a relatively short period around the mature phase. It is difficult to trace the origins of anomalies back in the transition phase. In order to obtain a more complete and robust picture of the evolution of DSV it is necessary to keep accumulating and archiving global SST and atmospheric data to the future.

**Acknowledgments.** The authors would like to thank colleagues at the International Pacific Research Center (IPRC), for their useful advice, comments, and suggestions. We are also grateful to the two anonymous reviewers for their valuable comments, which were quite helpful to improve the manuscript. The present work has been supported by the Institute for Global Change Research of the Frontier Research System for Global Change. This is the School of Ocean and Earth Science Technology (SOEST) contribution 5583 and IPRC publication 106.

## References

An, S.-L., and B. Wang, Interdecadal change of the structure of the ENSO mode and its impact on the ENSO frequency, *J. Clim.*, *13*, 2044–2055, 2000.

Balmaseda, M. A., M. K. Davey, and D. L. T. Anderson, Decadal and seasonal dependence of ENSO prediction skill, *J. Clim.*, *8*, 2705–2715, 1995.

Barnston, A. G., and R. E. Livezey, Classification, seasonality and persistence of low-frequency atmospheric circulation patterns, *Mon. Weather Rev.*, *115*, 1083–1126, 1987.

Cheng, X., G. Nitsche, and J. M. Wallace, Robustness of low-frequency circulation patterns derived from EOF and rotated EOF analyses, *J. Clim.*, *8*, 1709–1713, 1995.

Craddock, J. M., and C. R. Flood, Eigenvectors for representing the 500 mb geopotential surface over the Northern Hemisphere, *Q. J. R. Meteorol. Soc.*, *95*, 576–593, 1969.

Deser, C., and M. L. Blackmon, Surface climate variations over the North Atlantic Ocean during winter: 1900–1989, *J. Clim.*, *6*, 1743–1753, 1993.

Deser, C., and M. L. Blackmon, On the relationship between tropical and north Pacific sea surface temperature variations, *J. Clim.*, *8*, 1677–1680, 1995.

Fraedrich, K., C. Ziehmann, and F. Sielmann, Estimates of spatial degrees of freedom, *J. Clim.*, *8*, 361–369, 1995.

Ghil, M., and R. Vautard, Interdecadal oscillations and the warming trend in global temperature time series, *Nature*, *350*, 324–327, 1991.

Goddard, L., and N. E. Graham, El Nino in the 1990s, *J. Geophys. Res.*, *102*, 10,423–10,436, 1997.

Hamilton, K., A detailed examination of the extratropical response to the tropical El Niño/Southern Oscillation events, *J. Clim.*, *8*, 67–86, 1988.

Horel, J. D., and J. M. Wallace, Planetary-scale atmospheric phenomena associated with the Southern Oscillation, *Mon. Weather Rev.*, *109*, 813–829, 1981.

Hurrell, J. W., Decadal trends in the North Atlantic oscillation: Regional temperatures and precipitation, *Science*, *269*, 676–679, 1995.

Kachi, M., and T. Nitta, Decadal variations of the global atmosphere-ocean system, *J. Meteorol. Soc. Jpn.*, *75*, 657–675, 1997.

Kalnay, E., et al., The NCEP/NCAR 40-year reanalysis project, *Bull. Am. Meteorol. Soc.*, *77*, 437–471, 1996.

Kang, I.-S., Association of interannual and interdecadal variations of global-mean temperature with tropical Pacific SST appearing in a model and observations, *J. Clim.*, *9*, 455–464, 1996.

Kawamura, R., A rotated EOF analysis of global sea surface temperature variability with interannual and interdecadal scales, *J. Phys. Oceanogr.*, *24*, 707–715, 1994.

Kushnir, Y., Interdecadal variations in North Atlantic sea surface temperature and associated atmospheric conditions, *J. Clim.*, *7*, 141–157, 1994.

Latif, M., and T. P. Barnett, Causes of decadal climate variability over the North Pacific and North America, *Science*, *266*, 634–637, 1994.

Latif, M., R. Kleeman, and C. Eckert, Greenhouse warming, decadal variability, or El Nino? An attempt to understand the anomalous 1990s, *J. Clim.*, *10*, 2221–2239, 1997.

Lau, N.-C., and M. J. Nath, The role of the "atmospheric bridge" in liking tropical Pacific ENSO events to extratropical SST anomalies, *J. Clim.*, *9*, 2036–2057, 1996.

Livezey, R. E., and W. Y. Chen, Statistical field significance and its determination by Monte Carlo techniques, *Mon. Weather Rev.*, *111*, 46–59, 1983.

Mann, M. E., and J. Park, Spatial correlations of interdecadal variation in global surface temperatures, *Geophys. Res. Lett.*, *20*, 1055–1058, 1993.

Mann, M. E., and J. Park, Global-scale modes of surface temperature variability on interannual to century timescales, *J. Geophys. Res.*, *99*, 25,819–25,833, 1994.

Mantua, J. N., S. R. Hare, Y. Zhang, J. M. Wallace, and R. C. Francis, A Pacific interdecadal climate oscillation with impacts on salmon production, *Bull. Am. Meteorol. Soc.*, *78*, 1069–1080, 1997.

Meyers, S. D., A. M. Melson, G. T. Mitchum, and J. J. O'Brien, Detection of the fast Kelvin wave teleconnection due to El Niño–Southern Oscillation, *J. Geophys. Res.*, *103*, 27,655–27,663, 1998.

Minobe, S., A 50–70-year climatic oscillation over the North Pacific and North America, *Geophys. Res. Lett.*, *24*, 683–686, 1997.

Nakamura, H., and T. Yamagata, Oceans and climate shifts, *Science*, *281*, 1144, 1998.

Nakamura, H., and T. Yamagata, Recent decadal SST variability in the Northwestern Pacific and associated atmospheric anomalies, in *Beyond El Niño: Decadal and Interdecadal Climate Variability*, edited by A. Navarra, pp. 49–72, Springer-Verlag, New York, 1999.

Nakamura, H., G. Lin, and T. Yamagata, Decadal climate variability in the North Pacific during the recent decades, *Bull. Am. Meteorol. Soc.*, *78*, 2215–2225, 1997.

Nitta, T., and S. Yamada, Recent warning of tropical sea surface temperature and its relationship to the northern hemisphere circulation, *J. Meteorol. Soc. Jpn.*, *67*, 375–383, 1989.

Parker, D. E., C. K. Folland, and M. Jackson, Marine surface temperature: Observed variations and data requirements, *Clim. Change*, *31*, 559–600, 1995.

Rayner, N. A., E. B. Horton, D. E. Parker, C. K. Folland, and R. B. Hackett, Version 2.2 of the global sea-ice and sea surface temperature data set, 1903–1994, *Clim. Res. Tech. Note*, *74*, 1–21, 1996.

Robertson, A. W., C. R. Mechoso, and Y.-J. Kim, The influence of Atlantic sea surface temperature anomalies on the North Atlantic Oscillation, *J. Clim.*, *13*, 122–138, 2000.

Slingo, J. M., D. P. Rowell, K. R. Sperber, and F. Nortley, On the predictability of the interannual behavior of the Madden-Julian Oscillation and its relationship with El Niño, *Q. J. R. Meteorol. Soc.*, *125*, 583–609, 1999.

Sutton, R. T., and M. R. Allen, Decadal predictability of North Atlantic sea surface temperature and climate, *Nature*, *388*, 563–567, 1997.

Thompson, D. W. J., and J. M. Wallace, The Arctic Oscillation signature in the wintertime geopotential height and temperature fields, *Geophys. Res. Lett.*, *25*, 1297–1300, 1998.

Thompson, D. W. J., and J. M. Wallace, Annular modes in the extratropical circulation, part I, Month-to-month variability, *J. Clim.*, *13*, 1000–1016, 2000.

Tourre, Y. M., Y. Kushnir, and W. B. White, Evolution of interdecadal variability in sea level pressure, sea surface temperature, and upper ocean temperature over the Pacific Ocean, *J. Phys. Oceanogr.*, *29*, 1528–1541, 1999.

Trenberth, K. E., Recent observed interdecadal climate changes in the Northern Hemisphere, *Bull. Am. Meteorol. Soc.*, *71*, 988–993, 1990.

Trenberth, K. E., and J. W. Hurrell, Decadal atmosphere-ocean variations in the Pacific, *Clim. Dyn.*, *9*, 303–319, 1994.

Trenberth, K. E., and D. J. Shea, On the evolution of the Southern Oscillation, *Mon. Weather Rev.*, *115*, 3078–3096, 1987.

Wallace, J. M., and D. S. Gutzler, Teleconnections in the geopotential height field during the Northern Hemisphere winter, *Mon. Weather Rev.*, *109*, 784–812, 1981.

Wang, B., Interdecadal changes in El Nino onset in the last four decades, *J. Clim.*, *8*, 267–285, 1995.

Wang, B., and Y. Wang, Temporal structure of the Southern Oscillation as revealed by waveform and wavelet analysis, *J. Clim.*, *9*, 1586–1598, 1996.

Wang, J., and M. Ikeda, Arctic oscillation and Arctic sea-ice oscillation, *Geophys. Res. Lett.*, *27*, 1287–1290, 2000.

Watanabe, M., M. Kimoto, T. Nitta, and M. Kachi, A comparison of decadal climate oscillations in the North Atlantic detected in observations and a coupled GCM, *J. Clim.*, *12*, 2920–2940, 1999.

Weare, B. C., A. R. Navato, and R. E. Newell, Empirical orthogonal analysis of Pacific sea surface temperatures, *J. Phys. Oceanogr.*, *6*, 671–678, 1976.

White, W. B., and D. R. Cayan, Quasi-periodicity and global symmetries in interdecadal upper ocean temperature variability, *J. Geophys. Res.*, *103*, 21,335–21,354, 1998.

Xie, S.-P., and Y. Tanimoto, A pan-Atlantic decadal climate oscillation, *Geophys. Res. Lett.*, *25*, 2185–2188, 1998.

Zhang, R.-H., and S. Levitus, Structure and cycle of decadal variability of upper-ocean temperature in the North Pacific, *J. Clim.*, *10*, 710–727, 1997.

Zhang, X., J. Sheng, and A. Shabbar, Modes of interannual and interdecadal variability of Pacific SST, *J. Clim.*, *11*, 2556–2569, 1998.

Zhang, Y., and J. M. Wallace, Is climate variability over the North Pacific a linear response to ENSO?, *J. Clim.*, *9*, 1468–1478, 1996.

Zhang, Y., J. M. Wallace, and D. S. Battisti, ENSO-like interdecadal variability: 1900–93, *J. Clim.*, *10*, 1004–1020, 1997.

H. Nakamura, Department of Earth and Planetary Physics, University of Tokyo, 7-3-1 Hongo, Bunkyo-Ku, Tokyo 113-0033, Japan. (hisashi@geophys.u-tokyo.ac.jp)

T. Tomita, Frontier Research System for Global Change, Institute for Global Change Research, 3173-25 Showa-machi, Kanazawa-ku, Yokohama-shi, Kanagawa 236-0001, Japan. (tomita@jamstec.go.jp)

B. Wang, International Pacific Research Center, University of Hawaii at Manoa, 2525 Correa Road, Honolulu, HI 96822, USA.

T. Yasunari, Institute of Geoscience, University of Tsukuba, Tsukuba, Ibaraki 305-8571, Japan. (yasunari@atm.geo.tsukuba.ac.jp)

(Received August 29, 2000; revised June 7, 2001;
accepted June 15, 2001.)